

Specific Ionic Recognition Using Fig's Xylem/Phloem Vessel as a Novel and Applicable Device: Lab-on-a Xylem/Phloem

Nahid Maghsoudi and Mohammad Mahdi Doroodmand*

Cite This: *ACS Omega* 2022, 7, 20596–20604

Read Online

ACCESS |



Metrics & More

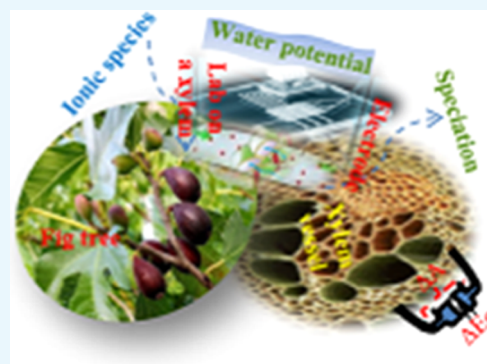


Article Recommendations



Supporting Information

ABSTRACT: A novel and specific detection system using voltage-stimulating ion transport through fig xylem/phloem vessels as a new lab-on-a xylem/phloem substrate was introduced. The voltage drove the ion flux through the vessels by a sinusoidal waveform with very low frequency (2.70 ± 0.05 kHz, $n = 10$) and voltage amplitude between 0.0 and 1.0 kV (vs total applied potential) with positive and negative polarities depending on cation and anion separation, respectively. The recorded potential induced by the applied potential was considered as a fingerprint electrical potential stimulator during reliable recognition of different ionic species. The system possessed some different characteristics such as (i) prominent figures of merit with linear ranges between 5.0 and 1200.0 (± 0.7 , $n = 10$) ng mL⁻¹ (correlation coefficient, R^2 , >0.99) for each ionic species and (ii) improved detection limits via tracing electrical current and conductance gradient (as the sensitive detection systems), while testing 50.0 ng mL⁻¹ of different salts as cationic and anionic species. The reliability of the system was evidenced via focusing on at least 60 independent cationic and anionic species during introducing a 70-membered distinct array-based bio-substrate device. This process not only showed great method applicability for specific determination with acceptable figures of merit but also resulted in introducing a software database for direct detection and recognition of various ionic analyses. The introduced detection/separation device competed with other spectroscopic/electrochemical systems due to the specific and simultaneous recognition of great ranges of ionic species in different real samples at ultratrace levels.



1. INTRODUCTION

Plants need to take water and other nutrients by routes and vessels for carrying even to the very long distance growing stem.¹ The basic paths in plant fluid transport are xylem and phloem, which are the main carrier of organic and inorganic materials. The phloem is responsible for transporting organic material from leaves (photosynthetic parts) or accumulated places to where it is needed.² This driving force is caused by a hydrostatic (turgor) pressure gradient that is osmotically drawn due to the transport of sap from sources to sink regions. The pressure occurring in live sieve tube pathways axially connected to each other causes mass flow transport.^{3,4} The xylem enables water and inorganic material translocation from soil to other parts of the plant, while the phloem does it for sugars and other organic substances.² This driving force is due to the water evaporation from leaves.

Materials and nutrition are translocated between the phloem and xylem by a vast exchange procedure in plant transport, especially in long-distance ones.⁵ Scientifically, the effective exchange between phloem and xylem causes a fundamental connection.⁶ Both xylem- and phloem-transporting vessels come together to form a vascular bundle in higher plants to connect the leaves, stalk, and roots, i.e., structural protection. In fact, they can be refined by themselves if these bundles are destroyed. Theoretically, this connection of xylem and phloem

depends on water potential equilibrium with surrounding apoplast that causes a hydraulic coupling.^{7,8}

In 1930, Minchin et al. described a hypothesis for osmotically driven phloem transport.³

Also, Stout with Hoagland in 1939 and Biddulph with Markle in 1944 proposed the phenomenon of solute transfer from xylem to phloem and vice versa.^{9,10} An in-depth study on the physiological properties of the radial transfer has been investigated for a few trees by Sauter in 1966.⁶

However, our knowledge about the exchange between xylem and phloem is still very limited. The mechanism behind this mass transfer involves diffusion (i.e., concentration gradient),¹¹ convection (due to the mechanical vibration and perturbation of some different parenchyma tissues),^{12–14} and migration (based on the water potential of the water medium inside the tree body).^{15,16} In this study, we inspired from the similarity of the quadrupole and dipole mass analyzer of mass spectrometry

Received: January 28, 2022

Accepted: May 17, 2022

Published: June 6, 2022



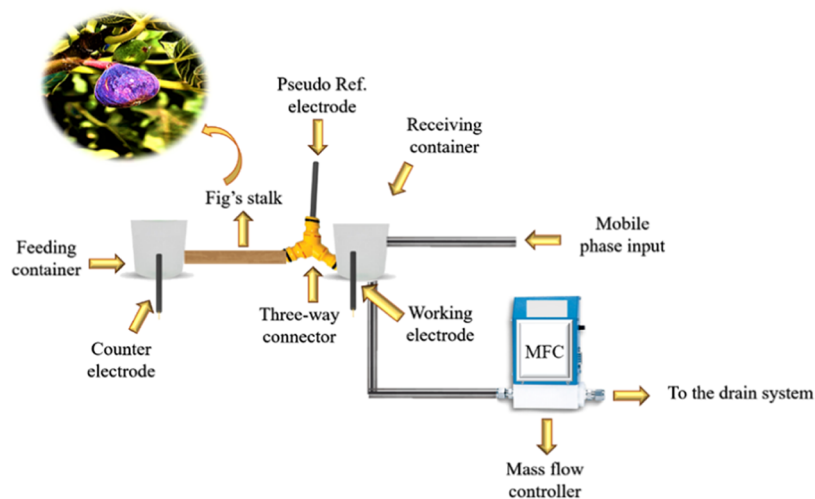


Figure 1. Schematic of the xylem/phloem bio-separator instrumentation system.

to xylem/phloem vessels of different plants, especially spongy parenchyma tissues such as the stem of a fig tree as a natural substrate ionic and molecular sieving system^{17,18} in the ion transport process.

To have a reliable detection/separation system, factors such as sensitivity, specificity, simplicity, portability, system miniaturizing, fast responding, etc. are important. However, there is little knowledge about such devices in the literature focused on a slice of a natural system such as a piece of fig stalk.¹⁹ Consequently, to operate the xylem/phloem vessels as a molecular/ionic sieving mass analyzer, controllable transport of water potential inside the tree organs is necessary.^{20,21}

Based on the literature, controlling and managing water potential as a kind of driving force can be achieved using some external stimulating forces such as magnetic field, gas purging, water-pumping, pressure-vacuuming, and electromagnetic potentials.^{22–25} However, most of these external forces suffer from irregular and uncontrollable mass transfer processes, especially in sensitive and thin films such as soft tissues. Also, formations of gas swelling due to water edema or vacuum-based shrinkages are another problem in controllable mass transfer.^{26,27}

In addition, the nonmagnetic property of tree tissues, besides their thickness, limits scientists to focus on the magnetic-based process even in qualitative or semiquantitative analysis inside such organs.^{28,29} Therefore, to have an applicable inductive electromagnetic force, it is necessary to use some “ferro/para” magnetic compounds such as Fe_3O_4 inside the xylem/phloem vessels following the magnetic flow gradients between the external force and the tissues.^{30,31} Besides, the presence of multiple pathways, especially inside tissues, dilutes the concentration of the magnetic particles and thus limits its applicability to obtain repeatable and controllable transportation/detection devices.^{32–34} These challenges made us concentrate on applying potential even by introducing an electrode system on tree stem tissues to obtain a well-defined detection system, specifically for a series of analytes.^{35–37}

It is hoped that the “harmonia” between the water potential as the selected function factor as well as the waveform, pulse amplitude, and electrical frequency of the applied potential make the tree stalk a natural ionic bio-transporting/separating system efficiently. Obviously, reaching these hypotheses would

encourage the analyst to introduce such detection systems. In this study, for the first time, specific ionic recognition using fig’s xylem/phloem vessel as an applicable substrate in a controllable separation/detection device is evaluated in detail.

2. EXPERIMENTAL SECTION

2.1. Materials and Solutions. To prepare stock solutions (50.0 ng mL^{-1}), different water-soluble salts with purity percentages between 98.0 and 99.9% (w/w), such as: KClO_3 , KClO_4 , $\text{BaCl}_2 \cdot 2\text{H}_2\text{O}$, $\text{Ce}(\text{NO}_3)_3 \cdot 6\text{H}_2\text{O}$, $\text{Ba}(\text{NO}_3)_2$, H_3BO_3 , $\text{Ba}(\text{CH}_3\text{COO})_2$, $\text{Ca}(\text{OH})_2$, $\text{CdSO}_4 \cdot 8\text{H}_2\text{O}$, $\text{L-C}_6\text{H}_8\text{O}_6$, K_2SO_4 , $\text{K}_2\text{Cr}_2\text{O}_7$, CaSO_4 , NaF , NaCl , Na_3PO_4 , NaHCO_3 , CaCl_2 , $\text{Ce}(\text{SO}_4)_2 \cdot 4\text{H}_2\text{O}$, $\text{CuCl}_2 \cdot 2\text{H}_2\text{O}$, KCl , NaH_2PO_4 , $\text{CH}_3\text{COONH}_4$, $\text{C}_6\text{H}_8\text{O}_7$, $\text{DL-C}_4\text{H}_6\text{O}_6$, KClO_3 , NaBr , NaNO_2 , $\text{Cd}(\text{NO}_3)_2 \cdot 4\text{H}_2\text{O}$ (Sigma-Aldrich), $\text{Na}_2\text{Cr}_2\text{O}_7 \cdot 2\text{H}_2\text{O}$, KNO_3 , $\text{Na}_2\text{B}_4\text{O}_7 \cdot 10\text{H}_2\text{O}$, $\text{NiCl}_2 \cdot 6\text{H}_2\text{O}$, $\text{Ni}(\text{NO}_3)_2 \cdot 6\text{H}_2\text{O}$, $\text{CoCl}_2 \cdot 6\text{H}_2\text{O}$, $\text{NaClO}_4 \cdot \text{H}_2\text{O}$, Na_2SO_3 , NaI , K_2CrO_4 , NaBrO_3 , KBrO_3 , $\text{Na}_2\text{C}_2\text{O}_4$, Na_2CO_3 , $\text{Na}_3\text{AsO}_4 \cdot 7\text{H}_2\text{O}$, $\text{Mg}(\text{NO}_3)_2 \cdot 6\text{H}_2\text{O}$, NaOH , AgNO_2 (Sigma-Aldrich), NaIO_4 , NaBH_4 , $\text{Na}_2\text{SeO}_3 \cdot 5\text{H}_2\text{O}$ (Sigma-Aldrich), $\text{Zr}(\text{NO}_3)_4$ (Sigma-Aldrich), Na_2BiO_3 , and $\text{Na}_2\text{S}_2\text{O}_3$ were individually prepared in 50.0 mL volumetric flasks, along with dilution to the mark with triple-distilled water (DI water, resistivity: of $17.8 \pm 0.5 \text{ m}\Omega \text{ cm}^5$, CAS: 7732-18-5/1848333-Millipore, Merck Company). Daily dilution of the stock solutions was achieved to prepare standard solutions between 1.0 and $5000.0 \text{ ng mL}^{-1}$. All of the mentioned reagents were purchased from the Merck Company.

Bleaching detergent (purity percentage: 35.0%, W/W) was related to Golrang Company (Tehran, Iran) as a source of ClO^- in stalk conditioning. The pH of the solution was adjusted between 4.0 and 10.0 (± 0.1) using HCl and NaOH (0.1 mol L^{-1} , Merck Company). The ionic strength of the solution was controlled using NaCl ($0.10 \pm 0.01 \text{ mol L}^{-1}$, Merck Company) standard solution. Analytical grades of organic solvents such as tetrahydrofuran (THF), acetone, 2-propanol, etc., with purity percentage $>99.0\%$ (W/W, analytical grade), were also purchased from Merck Company. It should be noted that, during the optimization process, for better comparison between the electrical potential gradients, the concentration units were based on molar scales. However, for the ionic determination and separation process, for more

suitable sample preparation, as well as for dealing with standard data, ng mL⁻¹ and μg mL⁻¹ units were selected.

To prepare the xylem/phloem vessel, a fig tree with characteristics such as sex: male, and year: below 2 years old from Shiraz, Iran (Shiraz University dormitory), was selected. The fig's wood stalk with different diameters between 0.5 and 2.5 (±0.1, *n* = 3) cm and various lengths between 1.0 and 10.0 (±0.1, *n* = 3) cm were cut using a wood hand saw (Hand Saw SK5 Japanese Saw three edge Teeth 65 HRC Wood Cutter for Tenon Wood Bamboo Plastic, crosscut hand saw: 620 mm, 24 in. long, China), with a 30 ± 2° angle and measured using a ruler (Vernier Caliper, 530 Series). A sampler (LC-4000 Series) was purchased from China and used for sampling the solutions. The sonication bath was a Codyson ultrasonic cleaner, 35 kHz, LavaDent, U.K.

2.2. Instrumentation. Poly(tetrafluoroethylene) (PTFE) containers were purchased from Thermo Fisher Scientific, U.K. A T-shaped flange (Water cooling PTFE three-way connector, dimension: 1.0 × 1.0 × 2.0 cm³, thread: general: G1/4, 10.0 mm i.d., Flagship) from Thermaltake Store, Taiwan, was used as a connector.

A PVC mechanical mass flow controller (PVC Mechanical Flow Control Valve) was purchased from Ranipet Shree Ghayathri Trading Private Limited | ID: 13561673733, China. The graphite rods were used as working, counter, and pseudo-reference electrodes (diameter: 4.0 ± 0.1 mm, length: 40.0 ± 0.1 mm) and bought from Hedong District, Tianjin, China. The potentiostat (7050-Electrochemical-Potentiostat/Galvanostat) was purchased from La Salle, 4-20132, Milano, Italy. The programmable function generator (MFG-2000 Series) and electronic read relays (Ngkc3C 5.0 V Normally Open Type Trigger Delay Switch Relay Module Relay Circuit Timing Alarm) were bought from China. A shift-register memory of an ST6C595 TSSOP16 Valor Electronic Components IC model was used to store each datum.

The ion-exchange chromatography equipment contained two cationic and anionic ion-exchange resin-based columns (20.0 ± 0.1 cm, Waters, with -COOH and -N(O-CH₃)₃⁺ functional groups, respectively) adopted as stationary phase and Datome-filled column (5.0 cm, Shimadzu, Japan) as guard column. The mobile phase included CH₃OH/H₂O (high-performance liquid chromatography, HPLC grade, 70.0:30.0%, V/V). The analytical process was achieved at 1100 ± 2 pass pressure and 25 °C temperature and buffer pH condition using phosphate buffer (0.01 mol L⁻¹, Merck Company). The suppressor module was used as a four-way alternative transmitting clocking pathways including ionic strength, pH buffer condition, mobile phase transition, and deionized water as the EC detector cleaner. The electrochemical conductivity probes (EC) were for Metrohm Company.

A high-performance liquid chromatograph (HPLC, Waters 600 via a Hamilton μ-syringe, 20.0 μL), an ultraviolet-visible (UV-vis) spectrometer (Jenway 7205 UV/Visible 72 Series Diode Array photodiode detector, PillPack—An Amazon Company), and a molecular fluorescence spectrometer (Varian) were selected as detection instruments. Every 5.0 min, a suitable volume of the receiving solution was sampled and introduced to these detection systems for tracing the mass transfer through the xylem/phloem vessels.

2.3. Designing Bio-System Based on Xylem/Phloem Vessel as a Separator/Transporter. The schematic of the fabricated instrumentation system is shown in Figure 1.

Table 1. Diffusion Coefficients Based on the Slope of the pH and Conductivity Values^a

feeding solution		receiving solution		time constant ^f (min)
matrix ^b	additives ^c (%)	matrix ^d	additives ^e (%)	
H ₂ O	HCl (2.0)	H ₂ O	HCl (2.0)	32
	NaOH (2.0)		HCl (5.0)	18
	NaCl (5.0)		NaOH (2.0)	27
	NaHCO ₃ (5.0)		NaOH (5.0)	38
THF	HCl (2.0)		HCl (2.0)	85
			HCl (5.0)	53
			HCl (10.0)	37
			HCl (20.0)	24
H ₂ O/THF (50:50, V/V)	HCl (2.0)		HCl (5.0)	91
	NaOH (2.0)			34
	NaCl (5.0)			15
	NaHCO ₃ (5.0)			52

^aThe data are the average of at least three independent analyses. ^b*V* = 15.0 mL. ^cAnalytical grades (W/W). ^d*V* = 15.0 mL. ^eAnalytical grade. ^fBased on percentage (W/W), estimated based on 90% of the steady-state condition (*t*₉₀), vs standard temperature and pressure (STP), ± standard deviation (SD). Conditions: fig's length: 2.0 ± 0.1 cm, diameter: 1.0 ± 0.1 cm.

As shown, the side arms of the fig stalk were connected to two identical containers (15.0 ± 0.1 mL) through a T-shaped flange. The first container was selected as the feeding solution in which the analyte or standard solution was introduced for quantitative/qualitative analysis. The second one has contained the receiving solution in which the transported ions are collected to be eluted by a laminar flow of triple-distilled water (flow rate of 2.0 mL min⁻¹) as the mobile phase following the drain. A PVC mechanical mass flow controller was used for adjusting the mobile phase flow rate.

First, before using the electrical potential in the instrument or controlling the mobile phase flow rate, to test the diffusion mass transfer, after elimination of the memory effect(s) of the fig stalk (see Section 2.4), the feeding and receiving containers were half-filled with the triple-distilled water (15.0 mL). Then, 1.00 mL of different water-soluble solvents such as THF, 2-propanol, various solutions, etc., with volume percentage between 20 and 30% (V/V) as standard solutions was individually introduced to the feeding solution, along with mixing using a mechanical stirrer with 300 ± 4 rpm for 2.0 h at room temperature. Then, detection systems such as pH glass electrode and EC (electrochemical conductivity) probes were introduced to the receiving vessel individually to measure the pH and electrochemical conductivity of the transported standard solution to the receiving container. The results are reported in progress for the transport rate of this phenomenon.

Also, to test this transport process, aqueous solutions (20.0 mL) containing 1.0 ± 0.1 mg L⁻¹ amino acids like tryptophan (>99.9%, Merck Company), tyrosine (99.0%, Flucka Company), L-arginine (>99.9%, Merck Company), and thymine (Aldrich Company) were adopted as the feeding solution. Then, their transport was traced inside the receiving solution via alternative (every 5.0 min) tests by the HPLC (UV-vis detector at λ between 210.0 and 300.0 ± 0.5 nm). The HPLC conditions included water/acetonitrile (70:30) as the mobile

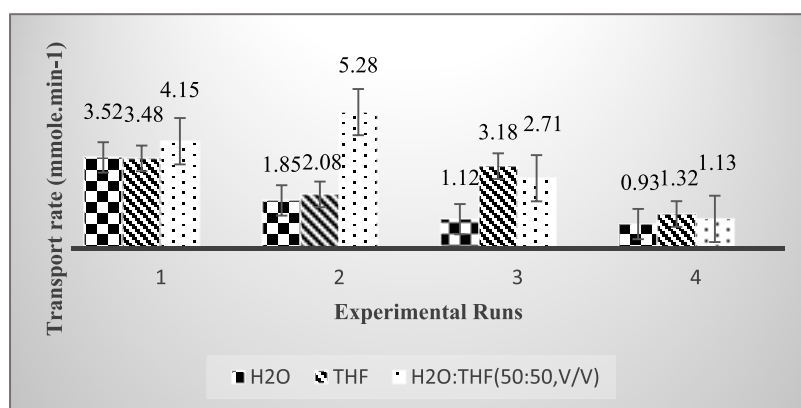


Figure 2. Diffusion coefficients based on the slope of the pH and conductivity values. (1) Data are the average of at least three independent analyses, (2) $V = 15.0$ mL, (3) analytical grades (W/W), (4) $V = 15.0$ mL, (5) analytical grade, (6) based on percentage (W/W), (6) estimated based on 90% of the steady-state condition (t_{90}), (7) averaged data at a fixed time constant ($t = 60.0 \pm 0.1$ min) vs standard temperature and pressure (STP), \pm : standard deviation (SD). Conditions: fig's length: 2.0 ± 0.1 cm, diameter: 1.0 ± 0.1 cm.

Table 2. Optimization by Simplex Method during the Analysis of K^+ and Cl^- Solutions ($1.0 \mu\text{g mL}^{-1}$) as a Selected Probes^a

vertex	fig wood		pH solution (± 0.01 , $n = 3$)	analytical potential (V, vs total applied potential, \pm standard deviation, $n = 3$)	output response	
	diameter, (cm, ± 0.1 , $n = 3$)	length, (cm, ± 0.1 , $n = 3$)			electrical current (mA, \pm standard deviation, $n = 5$)	electrical conductivity (μZ , \pm standard deviation, $n = 3$)
Condition: K^+ As Selected Probe. Response: Analytical Potential. Scan Rate: $+1.0 \text{ V s}^{-1}$						
1	0.8	2.0	7.0	2617.0 ± 0.3	8.3 ± 0.1	346.0 ± 0.1
2	0.8	2.7	3.1	912.0 ± 0.2	137.2 ± 0.2	918.0 ± 0.1
3	0.8	5.0	9.3	2318.0 ± 0.3	13.5 ± 0.1	483.0 ± 0.4
4	1.0	4.0	4.1	618.0 ± 0.1	153.8 ± 0.2	1317.0 ± 0.1
5	1.2	2.0	5.5	2519.0 ± 0.2	5.6 ± 0.2	208.0 ± 0.2
6	1.2	4.2	8.0	1736.0 ± 0.1	31.7 ± 0.1	732.0 ± 0.1
7	1.2	5.0	10.0	3814.0 ± 0.2	2.7 ± 0.1	173.0 ± 0.1
Condition: Cl^- As Selected Probe. Response: Analytical Potential. Scan Rate: -1.0 V s^{-1}						
1	0.8 ± 0.1	2.0 ± 0.1	7.0 ± 0.1	-2713.0 ± 0.3	-7.2 ± 0.1	324.0 ± 0.1
2	0.8 ± 0.1	2.7 ± 0.1	3.1 ± 0.1	-1035.0 ± 0.1	-125.8 ± 0.3	863.0 ± 0.3
3	0.8 ± 0.1	5.0 ± 0.1	9.3 ± 0.1	-2471.0 ± 0.2	-12.6 ± 0.1	421.0 ± 0.2
4	1.0 ± 0.1	4.0 ± 0.1	1.0 ± 0.1	-719.0 ± 0.3	-146.3 ± 0.3	1285.0 ± 0.1
5	1.2 ± 0.1	2.0 ± 0.1	5.0 ± 0.1	-2595.0 ± 0.1	-5.1 ± 0.1	182.0 ± 0.3
6	1.2 ± 0.1	4.2 ± 0.1	8.0 ± 0.1	-1812.0 ± 0.4	-27.8 ± 0.2	716.0 ± 0.1
7	1.2 ± 0.1	5.0 ± 0.1	10.0 ± 0.1	-3918.0 ± 0.1	-1.8 ± 0.1	137.0 ± 0.2

^aConditions: feeding and receiving volumes: 3.0 mL at room temperature.

phase (pressure: 1900 Psi, flow rate: 1.0 mL min^{-1}) and C-18 column (length: 20.0 cm) as the stationary phase.

2.4. Procedure. Prior to any analysis, to condition and also enlarge the fig stalk vessels, the H^+ ion at $\text{pH } 4.0 \pm 0.1$ was used during the introduction of 1.0 ± 0.1 mL of HCl and NaOH solutions ($0.10 \pm 0.01 \text{ mol L}^{-1}$). Then, 2 mL of the ClO^- solution with a 0.5% (V/V) concentration was introduced and sonicated for another 2.0 h at room temperature. After that, the containers were washed with distilled water entirely, and both of them were filled with water. Then, a sinusoidal voltage (vs total applied potential with a frequency of $2.70 \pm 0.05 \text{ kHz}$, $n = 10$) of 0.0 to +1.0 kV (for the cationic species) and 0.0 to -1.0 kV (for the anionic species) in a 5.0 min time interval was applied via the three-electrode system to eliminate any probable impurities and memory effect(s). After that, 3.0 mL of the analyte was introduced to the feeding container. Then, the electrical potentials were applied to the system through these three-electrode graphite rods as working, counter, and pseudo-reference electrodes. The electrical potential (direct/alternative currents, DC/AC) was applied between 0.0 and ± 1.0

kV (vs total applied potential) through a potentiostat. The amplitude of the electrical voltage was scanned in the range of +1.0 to -1.0 V s^{-1} (depending on the nature of the analyte with positive or negative charge, respectively) in the feeding solution to detect each ion-stimulating potential to transfer ions from feeding to receiving solution as well as detecting the electrical current and the EC gradients vs time in the receiving solution simultaneously.

Different electrical potential waveforms, such as square wave, triangular, normal pulses, differential pulse, $\sin(t)$, $\tan(t)$, $\tanh(t)$, etc., were generated by a programmable function generator to study more about this phenomenon. These waveforms were controlled through the PC via a software program written in Visual Basic 6 (VB6). Then, the electrical current was measured in the receiving container during individual migration of each ionic species along the fig stalk.

Electrical conductivity (EC) values were also measured via alternative switching of the modes of each reference and working graphite electrode between the EC two-electrode system using electronic on/off read relays.

Table 3. Figures of Merit during the Analysis of Different Water-Soluble Salts with a 1.0 $\mu\text{g mL}^{-1}$ Concentration (Some Solutions Were in Two Concentrations, 1.0 and 0.5 $\mu\text{g mL}^{-1}$)^a

row	water-soluble reagents			analytical potential (V, vs total applied potential, ± 0.1 V)			
	sample (1.0 \pm 0.1 $\mu\text{g mL}^{-1}$)	cation	anion	row	sample (1.0 \pm 0.1 $\mu\text{g mL}^{-1}$)	cation	anion
1	KClO ₃	148.7	-435.1	36	NaClO ₄ ·H ₂ O	127.5	-482.1
2	KClO ₄	152.5	-486.2	37	Na ₂ SO ₃	128.2	-331.6
3	BaCl ₂ ·2H ₂ O	217.1	-171.6	38	NaI	127.6	-228.2
4	Ce(NO ₃) ₃ ·6H ₂ O	452.2	-312.3	39	K ₂ CrO ₄	146.7	-512.5
5	Ba(NO ₃) ₂	219.0	-315.7	40	KIO ₃	147.5	-335.3
6	boric acid	335.4	-514.5	41	NaBrO ₃	131.4	-412.5
7	Ba(CH ₃ COO) ₂	214.3	-217.2	42	KBrO ₃	148.6	-414.2
8	NaF	131.5	-145.7	43	Na ₂ C ₂ O ₄	127.8	-381.1
9	NaCl	128.3	-171.1	44	Na ₂ CO ₃	131.3	-146.3
10	Na ₃ PO ₄	132.4	-392.5	45	NaAsO ₄ ·7H ₂ O	127.2	-471.3
11	NaHCO ₃	130.7	-169.2	46	Mg(NO ₃) ₂ ·6H ₂ O	273.6	-320.3
12	CaCl ₂	247.2	-175.5	47	NaOH	126.8	-132.1
13	K ₂ Cr ₂ O ₇	142.5	-712.3	48	AgNO ₂	418.2	-302.4
14	Ce(SO ₄) ₂ ·4H ₂ O	475.2	-346.7	49	NaIO ₄	131.3	-518.2
15	Ca(OH) ₂	248.9	-135.3	50	Na ₂ Cr ₂ O ₇ (0.5 \pm 0.1 $\mu\text{g/mL}$)	127.3	-872.4
16	CdSO ₄ ·8H ₂ O	482.3	-345.1	51	NaBH ₄	132.3	-351.1
17	L-ascorbic acid	83.4	-714.7	52	Na ₂ SeO ₃ ·5H ₂ O	128.7	-617.2
18	CoSO ₄	411.5	-345.3	53	Zr(NO ₃) ₄	507.1	-319.2
19	CuCl ₂ ·2H ₂ O	562.2	-173.7	54	NaBiO ₃	131.4	-735.3
20	KCl	151.6	-172.2	55	NaOH (0.5 \pm 0.1 $\mu\text{g/mL}$)	128.6	-137.1
21	NaH ₂ PO ₄	132.2	-383.7	56	Na ₂ S ₂ O ₈	132.0	-618.4
22	CH ₃ COONH ₄	154.7	-221.1	57	Ni(NO ₃) ₂ ·6H ₂ O	531.4	-318.1
23	K ₂ SO ₄	147.1	-348.8	58	K ₂ SO ₄	149.3	-348.3
24	citric acid	85.4	-412.3	59	Ca(OH) ₂	251.3	-126.2
25	KBr	151.7	-205.2	60	K ₂ Cr ₂ O ₇ (0.5 \pm 0.1 $\mu\text{g/mL}$)	147.2	-673.3
26	DL-tartaric acid	82.2	-731.7	61	KBr (0.5 \pm 0.1 $\mu\text{g/mL}$)	152.1	-208.3
27	NaBr	128.7	-210.2	62	KIO ₃ (0.5 \pm 0.1 $\mu\text{g/mL}$)	151.6	-518.1
28	NaNO ₂	128.3	-305.6	63	KCl (0.5 \pm 0.1 $\mu\text{g/mL}$)	153.2	-173.4
29	Cd(NO ₃) ₂ ·4H ₂ O	453.2	-315.1	64	NaCl (0.5 \pm 0.1 $\mu\text{g/mL}$)	131.1	-174.3
30	Na ₂ Cr ₂ O ₇	127.8	-532.5	65	NaBr (0.5 \pm 0.1 $\mu\text{g/mL}$)	127.4	-212.7
31	KNO ₃	148.5	-314.3	66	NaIO ₄ (0.5 \pm 0.1 $\mu\text{g/mL}$)	129.3	-485.1
32	NaB ₄ O ₇ ·10H ₂ O	129.1	-815.1	67	KIO ₃ (0.5 \pm 0.1 $\mu\text{g/mL}$)	147.2	-335.4
33	NiCl ₂ ·6H ₂ O	239.2	-169.3	68	KClO ₃ (0.5 \pm 0.1 $\mu\text{g/mL}$)	148.1	-457.3
34	Ni(NO ₃) ₂ ·6H ₂ O	535.7	-316.2	69	NaI (0.5 \pm 0.1 $\mu\text{g/mL}$)	132.4	-230.5
35	CoCl ₂ ·6H ₂ O	415.3	-171.4				

^aNote: the data are the average of three replicate analyses.

Each datum was stored in the shift-register random access memory and finally sent to a personal computer for further interpretation. The potential at which the electrical current or EC data were detected, named the “stimulating potential”, played a role as a “fingerprint” potential for each qualitative analysis.

Also, the quantitative test was achieved via alternatively switching the stimulating potential (vs total applied potential) between the fingerprint potential of H⁺ and the analyte with a 2.0 s resting time in the case of H⁺ ion ($+83.6 \pm 0.3$ V, vs total applied potential, $n = 3$). Then, the ratio of peak height or peak area (for both current and conductivity) of the analyte to H⁺ was measured.

2.5. Fig Bio-Array System. To estimate the reproducibility and also to have fast multiple analyses, a 70-membered array bio-separating system was fabricated and controlled through the electronic circuit. The data acquisition is stored in a shift-register memory by controlling through the software.

3. RESULTS AND DISCUSSION

3.1. Mass Transfer Process. Before applying a voltage to the stalk, to evaluate the mass transfer property with maximum rate, the effects of different mass transfer mechanisms such as diffusion and convection were evaluated in detail. For this purpose, four experiments were arranged using three electrolytes in feeding (F) (H₂O, THF, and H₂O/THF 50:50) and receiving (R) (H₂O) solution containers. The time constant was the required time to reach a constant maximum detection answer. The results are shown in Table 1.

Table 1 shows that, for example, in the third solution (H₂O/THF 50:50), after using HCl 2.0% in the feeding solution and HCl 5.0% in the receiving solution, with a time constant of about 90.0 min, maximum conductivity (mass transport) is achieved. The ultimate results for each experiment are shown in Figure 2.

Figure 2 shows that even for the maximum transport rate (5.28 ± 1.5 for solution H₂O/THF 50:50), we could not use a diffusion process to obtain an acceptable mass transport even after some hours for a simple electrolyte solution. So, it was

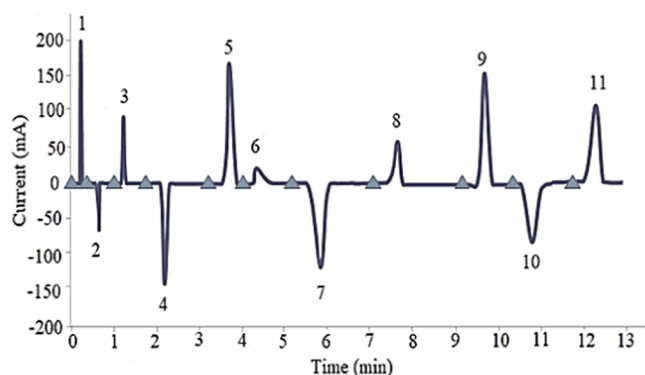


Figure 3. Current–time diagram during qualitative recognition of different cationic and anionic species with $1.0 \mu\text{g mL}^{-1}$ including (1) H^+ , (2) Cl^- , (3) Na^+ , (4) S^{2-} , (5) Fe^{2+} , (6) Fe^{3+} , (7) $\text{C}_2\text{O}_4^{2-}$, (8) Ca^{2+} , (9) Mg^{2+} , (10) CH_3COO^- , and (11) Ni^{2+} . Length: 2.0 ± 0.1 cm, diameter: 1.0 ± 0.1 cm, feeding and receiving volumes: 15.0 mL at room temperature. Triangular: switching-on and maximum peak height: switching-off of the analytical potentials based on the database.

decided to apply different conditions such as temperature, ultrasonic radiation, and pressure to improve the mass transfer process (see Figure S1a–d). The maximum transport rate of the diffusion/convection phenomenon in the best condition, $4.0 \pm 1.7 \text{ mmol}\cdot\text{min}^{-1}$, showed that even using pressure, temperature, or ultrasonic radiation cannot improve this transport significantly. For example, in Figure S1d, the temperature and ultrasonic radiation in feeding and receiving solutions were $25 \text{ }^\circ\text{C}$ and 5.0 kHz , respectively. But the pressure was 2.0 and 0.8 atm for feeding and receiving solutions, respectively. Under this condition, the maximum mass transport was about $2.8 \text{ mmol}\cdot\text{min}^{-1}$. As a result, none of the applied mass transport mechanisms can improve the rate of mass transport as well as the controllable one.

However, a very rapid mass transfer process has occurred when the electrical potential is applied by introducing the electrode to each container. This strongly revealed the importance and synergistic effect(s) of both diffusion and migration phenomena. Finally, the optimization process was performed during the application of the AC/DC triggering potential. The results pointed to the significance of the migration/diffusion mass transfer process for ionic transport through the fig stalk under the optimum condition.

3.2. Optimization. To obtain maximum sensitivity (i.e., the highest electrical current and electrochemical conductivity), different factors such as length and diameter of the fig stalk, pH of the feeding solution, fig stalk conditioning, etc. were optimized. This purpose was done by one-factor-at-a-time (see Figure S2) and Simplex (Table 2) method using K^+ and Cl^- as the selected probes. The limit of each factor was evaluated based on the priority of the influence on the sensitivity of the system. It is obvious that the less potential (and higher electrical current), the more acceptable condition for the designed instrument would obtain. As shown, although most of the items are in agreement, we can see that the length results are not in harmony in these two methods. For example, in the Simplex method (Table 2), the best optimum condition (less positive and less negative potentials for K^+ and Cl^- , respectively) was obtained at 4 cm and 1 cm for length and diameter, respectively, but in one-factor-at-a-time method

Table 4. Real Sample Analysis during Measuring Ca^{2+} , HCO_3^- , and Mg^{2+} by the Standard Addition Method and Ion-Exchange Chromatography^a

row	real sample	results ($\mu\text{g mL}^{-1}$)					
		introduced method		ion-exchange chromatography		maximum relative error percentage (%; $n = 3$)	
		Ca^{2+}	HCO_3^-	Mg^{2+}	Ca^{2+}	HCO_3^-	Mg^{2+}
1	drinking water	1.18 ± 0.12	58.15 ± 0.41	2.37 ± 0.18	1.23 ± 0.37	65.24 ± 0.63	27.10 ± 0.3
2	wastewater	45.93 ± 0.27	87.46 ± 0.34	57.83 ± 0.32	52.81 ± 0.72	89.17 ± 0.38	61.17 ± 1.72
3	well water	15.21 ± 0.32	82.15 ± 0.17	18.34 ± 0.52	14.24 ± 0.82	87.24 ± 0.31	15.71 ± 2.13
4	industrial water	537.43 ± 0.86	735.85 ± 0.34	719.35 ± 0.52	545.82 ± 0.27	745.72 ± 1.32	726.72 ± 2.17
5	plasma fluid	37.12 ± 0.35	27.12 ± 0.25	2.31 ± 0.53	42.15 ± 0.26	24.84 ± 0.54	2.08 ± 1.13
6	seawater	25.84 ± 0.13	35.52 ± 0.84	15.73 ± 0.35	23.52 ± 0.47	31.76 ± 0.52	17.31 ± 1.25
					4.00 ± 0.67	10.86 ± 0.52	12.54 ± 0.21
					13.01 ± 0.62	1.91 ± 0.32	5.46 ± 0.82
					6.81 ± 0.60	5.83 ± 0.26	16.74 ± 1.52
					1.50 ± 0.31	1.32 ± 0.33	1.01 ± 0.52
					12.33 ± 0.34	9.17 ± 0.45	11.05 ± 0.83
					9.86 ± 0.72	11.83 ± 0.72	9.12 ± 0.95

^aNote: data are the average of at least three replicate analyses. \pm : SD. Length: 2.0 ± 0.1 cm, diameter: 1.0 ± 0.1 cm, feeding and receiving volumes: 4.0 mL at room temperature.

Table 5. Comparison of the Introduced Method with Other Analytical Methods for K⁺ Ion Detections

row	factor	ion-exchange chromatography ³⁸	electrophoresis ³⁹	ICP ⁴⁰	flame-AAS ⁴⁰	current study
1	linear range ($\mu\text{g mL}^{-1}$)	0.1–1000.0		1.0–100.0	1.0–1000.0	5.0×10^{-3} –1.2
2	repeatability ($n = 4$, %)	0.03–0.32	0.7–2.3	<2	<2	2.47
3	reproducibility (% , $n = 3$)	1.81–2.10	4.0–10.0	< 0	<10	3.43
4	response time (t_{90} , s)	300.0	300.0		120–240	<10 s
5	resolution (kV) ($\pm\Delta V$, vs total applied potential)		20.0	100 ns		potential dependent
6	detection limit ($X_b + 3S_b$, $\mu\text{g mL}^{-1}$)	3.0	33.4×10^{-3}	1.0	6.0	1.8×10^{-5}

(Figure S2), this would be achieved at 2 cm length and 1 cm diameter.

Due to the impressive difference (K^+ : 618 and 250 V; Cl^- : –719 and –250 V in Simplex and one-factor-at-a-time method, respectively), it was decided to choose the one-factor-at-a-time method at lower potentials to continue the experiment.

It should be noted that the different pathways and complexity of these stalks as a natural system have made us to condition the stalks and also to use H^+ as the “internal switching probe” to obtain the peak area or peak height ratios for better reproducibility and also lower potential. In this process, the corresponding stimulating potentials of analyte and H^+ ions within a selected resting time with a 1.0 s pulse width in the case of H^+ ion ($+83.6 \pm 0.3$ V, vs total applied potential, $n = 3$; see embedded database) were sequentially applied. The peak height as well as the peak area ratios of analyte to H^+ , for both current and conductivity, were measured afterward. As a result, an impressive improvement was observed in both repeatability and reproducibility of the analytical signals.

This elucidated the potential of the current study for estimating the effective parameters as well as their interactions in the xylem/phloem vessels system in a kind of mimicking bio-sensing probe for reliable detection and determination of different types of anions and cations under optimum conditions.

3.3. Figures of Merit. The stimulating electrical analytical potentials of different ionic species are shown in Table 3.

As clearly shown (Table 3), a significant difference between the applied triggering potentials strongly revealed the selectivity of the detection system for trace and ultratrace detection of different forms of the cationic and anionic species. This characteristic showed the harmony of the fig stalk as a spongy parenchyma substrate for a fine mass transfer of the ionic species without any significant interference(s).

3.4. Qualitative Aspect for Ionic Species Recognition Purpose. A high enough difference between the fingerprint analytical potentials revealed the specificity of this bio-system for the ionic species recognition purpose. Based on the estimated analytical potentials, the current–time diagram during qualitative recognition of different standard cationic and anionic species with a $1.0 \mu\text{g mL}^{-1}$ concentration is shown in Figure 3.

3.5. Real Sample Analysis. The reliability of this method was evaluated via analysis of different real samples including drinking water (municipal tap water, Eram region, Shiraz, Iran), wastewater (Dry river, Marvdasht, Iran), well water (Marvdasht well water, Shiraz, Iran), industrial water (Golgohar Company, Kerman, Iran), human plasma fluid (Medical Shiraz, University, Shiraz, Iran), and seawater (Bushehr gulf, Iran). The real samples were collected around November 2020. The comparison with ion chromatography as

a standard method was carried out under similar conditions. For this purpose, each solution was sampled ($100.0 \mu\text{L}$) and diluted 100 times by the deionized water and filtered using a sintered glass Buchner funnel. The cations and anionic species were then simultaneously analyzed by the ion chromatography equipment for analysis and declaration of the probable mechanistic process according to the procedure reported in an ASTM (American Society for Testing and Material) international guideline. The results related to the real sample analysis for Ca^{2+} , HCO_3^- , and Mg^{2+} ions are shown in Table 4 and compared to the ion-exchange chromatography as a standard separation/detection system.

The results pointed to the reliability of the detection system for rapid and intelligent detection of different forms of ionic species. It should be noted that the detection limit was measured with the $S_b + 3\sigma_b$ formula.

3.6. Comparison. A comparison between the introduced bio-system and some other analytical methods is shown in Table 5.

As clearly shown, in the detection system, major advantages such as simplicity, rapid analysis, and high selectivity for the analysis of different ionic species are apparent.

4. MECHANISM

In this method, the principle of separation and detection is vessel-based transformation that happens through the stalk in a specific triggering potential. It was observed that water oxidation and reduction happened to produce O_2 and H_2 gases in each side of the stalk (receiving and feeding container), respectively. These observations were confirmed by the GC-TCD method. In fact, this happened in the containers, at the edge of the stalk, not inside it. If so, bubble production would close the path and fluidic mass transfer will not happen. Consequently, the oxidation/reduction did not occur or less occurred inside the stalk and the water potential production generates an electrophoretic force to pass the cation/anion specifically afterward. Depending on the ions produced by the water oxidation/reduction, the charge balance occurred during mass transfer. If the solution had no charge balance, the transfer number (t) caused a large potential difference on both sides, but it did not logically and experimentally happen.

5. CONCLUSIONS

The introduced detection system is considered a notably analytical device for the selective and applicable detection of different ionic species in voltage triggering. This process is related to the simultaneous effectiveness of the applied potential and natural behavior of fig stalk as a spongy parenchyma tissue during the analysis of ionic compounds. To the best of our knowledge, this bio-system is considered the first report for the analytical species with high enough

availability, sensitivity, selectivity, eco-friendliness, and short analysis time.

■ ASSOCIATED CONTENT

SI Supporting Information

The Supporting Information is available free of charge at <https://pubs.acs.org/doi/10.1021/acsomega.2c00589>.

Diffusion/convection coefficients based on the slope of the pH and conductivity values (Figure S1) and one-factor-at-a time optimization of K⁺ and Cl⁻ ions (Figure S2) (PDF)

■ AUTHOR INFORMATION

Corresponding Author

Mohammad Mahdi Doroodmand – Department of Chemistry, College of Sciences, Shiraz University, Shiraz 71454, Iran; orcid.org/0000-0002-6142-8540; Phone: +98-71-36137152.; Email: Doroodmand@shirazu.ac.ir, Doroodmand@yahoo.com; Fax: +98-71-36460788

Author

Nahid Maghsoudi – Department of Chemistry, College of Sciences, Shiraz University, Shiraz 71454, Iran

Complete contact information is available at:

<https://pubs.acs.org/doi/10.1021/acsomega.2c00589>

Author Contributions

M.M.D. directed the research group, supported the necessary methods, and edited the manuscript. N.M. performed all of the electrical experiments, consulted the project, analyzed the data, and wrote and edited the manuscript. Dr. Morteza Akhound further edited the final manuscript.

Funding

This study was financially supported by Shiraz University.

Notes

The authors declare no competing financial interest. This study was admitted and approved by the ethics committee of the Shiraz University Consul.

■ ACKNOWLEDGMENTS

The authors are extremely grateful to Shiraz University Research Council for its support in putting together this volume knowledge.

■ REFERENCES

- (1) Kumar, S.; Meena, R. S.; Jhariya, M. K. *Resources Use Efficiency in Agriculture*, Springer, 2020.
- (2) Grof, C. P. L.; Byrt, C. S.; Patrick, J. W. *Phloem Transport of Resources*, Wiley, 2013.
- (3) Hölttä, T.; Mencuccini, M.; Nikinmaa, E. Linking phloem function to structure: analysis with a coupled xylem–phloem transport model. *J. Theor. Biol.* **2009**, *259*, 325–337.
- (4) Milburn, J. A. *Water Flow in Plants*; Longman Inc.: United Kingdom, 1979; p 151.
- (5) White, P. J. Long-Distance Transport in the Xylem and Phloem. In *Marschner's Mineral Nutrition of Higher Plants*, Elsevier, 2012; pp 49–70.
- (6) Van Bel, A. J. E. Xylem-phloem exchange via the rays: the undervalued route of transport. *J. Exp. Bot.* **1990**, *41*, 631–644.
- (7) Thomas, B. *Encyclopedia of Applied Plant Sciences*, 2nd ed.; Academic Press, 2016.
- (8) Thompson, M. V.; Holbrook, N. M. Scaling phloem transport: water potential equilibrium and osmoregulatory flow. *Plant, Cell Environ.* **2003**, *26*, 1561–1577.
- (9) Stout, P. R.; Hoagland, D. R. Upward and lateral movement of salt in certain plants as indicated by radioactive isotopes of potassium, sodium, and phosphorus absorbed by roots. *Am. J. Bot.* **1939**, *26*, 320–324.
- (10) Biddulph, O.; Markle, J. Translocation of radiophosphorus in the phloem of the cotton plant. *Am. J. Bot.* **1944**, *31*, 65–70.
- (11) Wang, X.; Liu, Z.; Pang, Y. Concentration gradient generation methods based on microfluidic systems. *RSC Adv.* **2017**, *7*, 29966–29984.
- (12) Shah, D. U.; Reynolds, T. P. S.; Ramage, M. H. The strength of plants: theory and experimental methods to measure the mechanical properties of stems. *J. Exp. Bot.* **2017**, *68*, 4497–4516.
- (13) Armstrong, W.; Armstrong, J. Plant Internal Oxygen Transport (Diffusion and Convection) and Measuring and Modelling Oxygen Gradients. In *Low-Oxygen Stress in Plants*, Springer, 2014; pp 267–297.
- (14) Braam, J. In touch: plant responses to mechanical stimuli. *New Phytol.* **2005**, *165*, 373–389.
- (15) Papendick, R. I.; Campbell, G. S. Theory and Measurement of Water Potential. In *Water Potential Relations in Soil Microbiology*, American Society of Agronomy, 1981; Vol. 9, pp 1–22.
- (16) Dileanis, P. D.; Groeneveld, D. P. *Osmotic Potential and Projected Drought Tolerance of Four Phreatophytic Shrub Species in Owens Valley*; USGPO: California, 1989.
- (17) Schweingruber, F. H.; Börner, A. *The Plant Stem: A Microscopic Aspect*, Springer, 2018.
- (18) Mawa, S.; Husain, K.; Jantan, I. *Ficus carica L. (Moraceae): Phytochemistry, traditional uses and biological activities. Evid.-Based Complement. Altern. Med.* **2013**, *2013*, No. 974256.
- (19) Yaman, B. Anatomical differences between stem and branch wood of *Ficus carica L. subsp. carica*. *Mod. Phytomorphol.* **2014**, *6*, 79–83.
- (20) Spicer, R. Symplasmic networks in secondary vascular tissues: parenchyma distribution and activity supporting long-distance transport. *J. Exp. Bot.* **2014**, *65*, 1829–1848.
- (21) Zabel, R. A.; Morrell, J. J. *Wood Microbiology: Decay and Its Prevention*, Academic Press, 2012.
- (22) Gieling, T. H. Control of Water Supply and Specific Nutrient Application in Closed Growing Systems, 2001.
- (23) Dursun, B.; Gokcol, C. The role of hydroelectric power and contribution of small hydropower plants for sustainable development in Turkey. *Renewable Energy* **2011**, *36*, 1227–1235.
- (24) Robbins, N. E.; Dinnyen, J. R. Growth is required for perception of water availability to pattern plant root branches. *Proc. Natl. Acad. Sci. U.S.A.* **2018**, *115*, E822–E831.
- (25) Goto, E.; Kurata, K.; Hayashi, M.; Sase, S. In *Plant Production in Closed Ecosystems*. The International Symposium on Plant Production in Closed Ecosystems, Narita, Japan, August 26–29, 1996; 2013.
- (26) Eichler, S.; Ramon, O.; Cohen, Y.; Mizrahi, S. Swelling and contraction driven mass transfer processes during osmotic dehydration of uncharged hydrogels. *Int. J. Food Sci. Technol.* **2002**, *37*, 245–253.
- (27) Ahmed, E. M. Hydrogel: Preparation, characterization, and applications: A review. *J. Adv. Res.* **2015**, *6*, 105–121.
- (28) Zang, Z.; Wang, J.; Cui, H-L.; Yan, S. Terahertz spectral imaging based quantitative determination of spatial distribution of plant leaf constituents. *Plant Methods* **2019**, *15*, No. 106.
- (29) van Dusschoten, D.; Ralf, M.; Johannes, K.; Johannes, A.; Postma, D. P.; Jonas, B.; Ulrich, S.; Siegfried, J. Quantitative 3D analysis of plant roots growing in soil using magnetic resonance imaging. *Plant Physiol.* **2016**, *170*, 1176–1188.
- (30) Pariona, N.; Martinez, A. I.; Hdz-Garcia, H. M.; Cruz, L. A.; Hernandez-Valdes, A. Effects of hematite and ferrihydrite nanoparticles on germination and growth of maize seedlings. *Saudi J. Biol. Sci.* **2017**, *24*, 1547–1554.

(31) Su, Y.; Caroline, K.; Venassa, A.; Adeyemi, S. A.; Philippe, R.; Caroline, R.; Jason, W.; David, J. Delivery, uptake, fate, and transport of engineered nanoparticles in plants: a critical review and data analysis. *Environ. Sci.: Nano* **2019**, *6*, 2311–2331.

(32) Abbas, Q.; Yousaf, B.; Ali, M. U.; Ahmed, M. M. A.; Jörg, R.; Naushad, Mu., et al. Transformation pathways and fate of engineered nanoparticles (ENPs) in distinct interactive environmental compartments: A review. *Environ. Int.* **2020**, *138*, No. 105646.

(33) Sarraf, M.; Kataria, S.; Taimourya, H.; Santos, L. O.; Menegatti, R. D.; Renata, D. M.; Jain, M.; Ihtisham, M.; Liu, S. Magnetic field (MF) applications in plants: An overview. *Plants* **2020**, *9*, 1139.

(34) Maffei, M. E. Magnetic field effects on plant growth, development, and evolution. *Front. Plant Sci.* **2014**, *5*, 445.

(35) Aslam, S.; Jennions, I. K.; Samie, M.; Perinpanayagam, S.; Fang, Y. Ingress of Threshold Voltage-Triggered Hardware Trojan in the Modern FPGA Fabric—Detection Methodology and Mitigation. *IEEE Access* **2020**, *8*, 31371–31397.

(36) Beer, A. C.; Weber, E. R.; Willardson, R. K.; Kiehl, R. A.; Sollner, T. C. L. G. *High Speed Heterostructure Devices*, Academic Press, 1994.

(37) Liu, H. C.; Sollner, T. High-frequency resonant-tunneling devices. *Semicond. Semimet.* **1994**, *41*, 359.

(38) Polite, L. N.; Mcnair, H. M.; Rocklin, R. D. Linearity in ion chromatography. *J. Liq. Chromatogr.* **1987**, *10*, 829–838.

(39) Flanigan, P. M., IV; Ross, D.; Shackman, J. G. Determination of inorganic ions in mineral water by gradient elution moving boundary electrophoresis. *Electrophoresis* **2010**, *31*, 3466–3474.

(40) da Silva, J. A. T.; Dobránszki, J. Magnetic fields: how is plant growth and development impacted? *Protoplasma* **2016**, *253*, 231–248.